



A New Zinc-based Metal Organic Framework as a Stationary Phase for Thin Layer Chromatography

Mouhammad Abu Rasheed^{1*}, Ahmad Alshaghel² and Amir Alhaj Sakur¹

¹Department of Food and Analytical Chemistry, Faculty of Pharmacy, University of Aleppo, Syria.

²Department of Chemistry, Faculty of Sciences, University of Aleppo, Syria.

Authors' contributions

This work was carried out in collaboration among all authors. Author MAR performed the experiments, put the characterization protocols and wrote the first draft of the manuscript. Author AA put the protocols for the organic synthesis and contribute to the experiments. Author AAS managed the project in all stages, contribute to the interpretation of data and revised the manuscript. All authors read and approved the final manuscript.

Article Information

DOI: 10.9734/IRJPAC/2020/v21i1030213

Editor(s):

(1) Dr. Li Cai, University of South Carolina Lancaster, South Carolina.

Reviewers:

(1) Janmajoy Banerjee, Gitanjali College of Pharmacy, Affiliated To Makaut, India.

(2) Subhasish Chaudhuri, Forensic Science Laboratory and Research Institute, India.

Complete Peer review History: <http://www.sdiarticle4.com/review-history/58911>

Original Research Article

Received 02 May 2020
Accepted 08 July 2020
Published 13 July 2020

ABSTRACT

Metal organic frameworks (MOFs) are a variety of micro-porous materials which have high surface area, and permanent porosity making them possible options as chromatographic stationary phases. Herein we reported the synthesis and characterization of a new MOF structure and its utilization as a stationary phase for thin layer chromatography (TLC). $[Zn(BMAB).DMF]_n$ is a zinc-based MOF with an organic linker consists of chemically distinct binding groups which is 4-[(1h-1,2,3-benzotriazol-1-yl)methyl]amino}benzoic acid (BMAB). This MOF was synthesized using ultra sound assisted reaction process, then activated via solvent exchange protocol to preserve its porous structure. FT-IR, UV-diffuse reflection spectroscopy (UV-DRS) and differential scanning calorimetry (DSC) were performed to characterize the synthesized MOF. Integrated data from "loss on desolvation" and atomic absorption spectrophotometry (AAS) measurements were used to define the chemical composition of the synthesized material. A specific surface area of 122.9 m²/g was determined for the activated MOF using methylene blue langmuir isotherm method. TLC plates were prepared from the activated form of the structure to investigate its chromatographic characteristics by utilizing it to separate a model mixture of benzidine and o-tolidine using n-propanol: Chloroform:

*Corresponding author: E-mail: mouhammed94a.b@hotmail.com;

Acetonitrile (50:30:20, v/v/v) as a mobile phase. The retardation factors (R_f), separation factor, and resolution (R_s) were determined via densitometric method at 310 nm to be 0.45 and 0.63 ($\alpha=2.08$, $R_s=1.61$) for o-tolidine and benzidine; respectively. The plate was then visualized using iodine chamber method to confirm a successful separation.

Keywords: Metal Organic Framework (MOF); Thin Layer Chromatography (TLC); stationary phase; micro-porous material; Differential Scanning Calorimetry (DSC); Specific Surface Area (SSA); Atomic Absorption Spectroscopy (AAS); N,N-Di Methyl Formamide (DMF).

1. INTRODUCTION

Developing new stationary phases for chromatographic techniques is of paramount importance in order to expand their applications and improve sensitivity and selectivity parameters. In this area, thin layer chromatography (TLC) is preferable as a primary technique to evaluate new stationary phases, as it is considered less demanding and more rapid [1]. Besides, the incorporation of densitometric measurements in TLC makes it more appropriate for quantitative evaluation [2].

Metal Organic Frameworks (MOFs), also known as Metal Organic Coordination Networks (MOCNs), are a group of advanced micro-porous polymers that consist of metal ions act as connectors linking the organic ligands via metal-ligand bonds to form the final structure [3]. The part of the structure where the metal ions are locked into position by forming mono- or poly-nuclear complexes with the active part of the organic linker is referred to as Secondary Building Unit (SBU). This hybrid cluster determines the direction and capacity of reticulation to produce a specific structure [4]. When it comes to the organic ligands, the majority of them consist of homogenous multi-dentate organic linkers, which can be anionic (like dicarboxylate ligands), cationic (such as triazole-based linkers), or neutral [5]. However, a few interest has been made to utilize linkers with heterogeneous binding groups [6,7].

Most of these MOF structures are known to have high surface area, permanent porosity and high thermal and solvents stability. These characteristics make it possible to utilize MOFs in various applications including chromatographic techniques [8]. Several metal organic frameworks have been used successfully as stationary phases in High Performance Liquid Chromatography (HPLC) [9–12] and Gas chromatography (GC) [13–16]. However, to the best of our knowledge, only one MOF structure has been reported in the literature as a TLC stationary phase under the name DUT-67 [17].

In this article, the synthesis and characterization of a new zinc based MOF are reported. $[Zn(BMAB).DMF]_n$ is described as pale white, hydrophobic crystalline powder, which was synthesized using Ultra-sound assisted reaction procedure in N,N-Di methyl formamide-Water solvent system. Several techniques were employed to characterize the resultant MOF. In addition to FT-IR, and DSC, which are usually reported as MOF characterizing techniques, diffuse reflection spectroscopy in the UV range (UV-DRS) was also utilized. The latter technique has been poorly reported for this purpose [18], but was used in this work to characterize the MOF structure and monitor the desolvation process. "Loss on desolvation" and AAS measurements were also applied for the first time to define the chemical composition of the synthesized MOF as $[Zn(BMAB).DMF]_n$. TLC plates were prepared from this material to study its chromatographic characteristics by employing them to separate a model mixture of benzidine and o-tolidine.

2. EXPERIMENTAL DETAILS

2.1 Materials

1H-Benzotriazole 98%, formaldehyde solution 37 wt. %, nitric acid 66%, and methylene blue.XH₂O (X=2–3) were supplied from Sigma-Aldrich, Germany. p-aminobenzoic acid 99%, and Hydrogen peroxide 27% from Alfa-Aesar, USA. N,N-Dimethylformamide (DMF) 98%, and Potassium hydroxide pellets 85% were supplied from Rectapur Prolabo, EEC. Zink nitrate hexahydrate $[Zn(NO_3)_2 \cdot 6H_2O]$ 99% pure from Riedel-de Haen AG, Germany. Methanol, isocratic HPLC grade from Scharlab S.L., Spain. Acetonitrile and ethanol, gradient grade for Liquid Chromatography, Merck KGaA, Germany. n-hexane 95% HPS grade for HPLC, n-propanol 99% chemically pure, and Iodine 99.5% were supplied from Surechem products LTD., England. Chloroform 98.5% from POCH SA, Poland. Benzidine base research grade, and o-

tolidine analytical grade from Serva, Heidelberg, Germany.

2.2 Apparatus

Elma Transsonic TI-H 10, sonication power 200 W (Elma Schmidbauer GmbH, Germany) was used for the synthesis of BMAB ligand and MOF material. NEY M-525 Series 2 oven (Yucaipa CA, USA) was used for drying, thermal activation, and "Loss on Desolvation" processes. FT-IR spectra were recorded on Jasco FT/IR-4200. Shimadzu "dual wavelength flying spot scanning" densitometer CS-9301 PC (Tokyo, Japan, 2000) (program version 2.00) was used for UV-DRS scanning and densitometric measurements of the plates after separation. Thermal measurements were conducted using Linseis DSC-PT10 for both activated and inactivated MOF. T70 UV/VIS Spectrometer (PG instruments) was used for spectrophotometric measurements to calculate the specific surface area. Phoenix-986 AAS, Sedico LTD. Was used for zinc determinations. Camag TLC plate coater (hand operated) was used to prepare TLC plates. Hamilton 1- μ L micro-syringe (Germany) was used to apply samples on TLC plates. Wheaton Hellendahl Staining Dish (7.5 \times 2.5 \times 7.5 cm) was used as a TLC developing chamber.

2.3 Synthesis of the Organic Linker

The synthesis of 4-[[1H-1,2,3-Benzotriazole-1-yl)methyl]amino]benzoic acid (BMAB) (Mw=268.27 g/mol) (Fig. 1) was performed using the ultra-sound assisted method described by Alshaghel [19]. 1.19 g (10 mmol) of 1H-benzotriazole and 1.37 g (10 mmol) p-aminobenzoic acid were dissolved in 10 mL ethanol:H₂O (2:1, v/v) solvent system, and sonicated for 5 mins. at 35 KHz. Frequency. Then 0.9 mL (~10 mmol) of formaldehyde solution was added. The mixture was sonicated for another 5 mins. at the same frequency. After that, the white precipitate was filtered, washed

with water, recrystallized in ethanol:H₂O (2:1, v/v), and dried at 70°C. (m.p.= 198-200°C).

2.4 Synthesis of [Zn(BMAB).DMF]_n

The synthesis of [Zn(BMAB).DMF]_n was performed using sonochemical method. 0.4 g (1.49 mmol) of the organic linker and 0.44 g (1.49 mmol) of Zn(NO₃)₂.6H₂O were dissolved separately in 15 mL DMF and 35 mL deionized water; respectively. The two solutions were mixed together in a round bottom flask, and then sonicated for 30 mins. after adding 0.04 g (0.745 mmol) of KOH. The white precipitate was filtered, washed twice with DMF, water, and methanol, and dried at 40°C for 1 hr., and then at 120°C for 2 hrs.

2.5 Activation of [Zn(BMAB).DMF]_n

The activation (desolvation) of the above synthesized MOF was performed using solvent exchange method [20]. In a well-closed glass tube, dried MOF was immersed in 5 mL n-hexane for 3 days, with the solvent being centrifuged and renewed every day. After that, the powder was placed under vacuum at 200°C for 3 hrs. to be completely desolvated.

2.6 TLC Plates Preparation and Chromatographic Conditions

Glass slides (7.5 \times 2.5 cm) were used to prepare TLC plates of 100 μ m thickness using Camag TLC plate coater. This process achieved by pouring a concentrated suspension of the activated MOF in n-hexane (1 g/10 mL). TLC plates were dried at 120°C for 1 hr.

A mixture solution of 1 mg/mL Benzidine and o-tolidine in methanol were prepared. 2 μ L-spot of this solution was applied to the prepared plate and developed using a mixture of n-propanol:chloroform:acetonitrile (50:30:20, v/v/v)

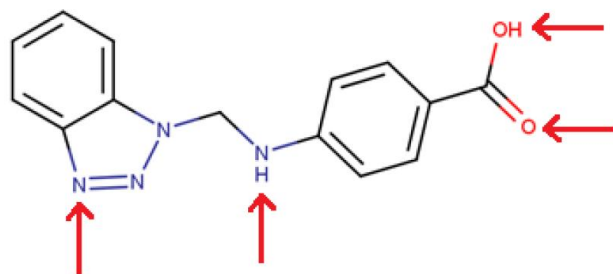


Fig. 1. The chemical structure and the binding groups of the organic linker BMAB

as a mobile phase. The mobile phase was let to develop for 5 cm then the plate was dried and densitometric measurements were applied to determine the retardation factors (R_f) at $\lambda = 310$ nm (linear, reflection mode). Next, the plate was incubated in an iodine chamber for 10 min. to visually confirm the separation.

3. RESULTS AND DISCUSSION

$[\text{Zn}(\text{BMAB})\cdot\text{DMF}]_n$ was synthesized using simple ultra-sound assisted method. Different ratios of the solvent system ($\text{H}_2\text{O}:\text{DMF}$) were used, with the ratio of (70:30, v/v) gave the highest yield. The synthesized MOF showed high hydrophobic characteristics, high surface area, and good thermal stability confirmed by multiple characterizing techniques. However, it revealed low stability just upon synthesis, as the first step of drying in no more than 40°C was necessary. Also, it showed poor chemical stability in acidic ($\text{pH}<3$) and alkaline ($\text{pH}>9$) solutions detected by significant changes occurred in samples' weight and FT-IR spectra after incubation (Fig. 2); respectively.

3.1 Characterization of $[\text{Zn}(\text{BMAB})\cdot\text{DMF}]_n$

The FT-IR spectrum observed for the synthesized organic ligand was identical with the literature spectrum [19]. By comparing FT-IR spectra for the organic linker and the synthesized MOF (Fig. 2), the strong broad band in the range of $3500\text{--}2500\text{ cm}^{-1}$ that refers to --COOH group in BMAB [21] was absent in MOF spectrum, where just a little broad band at 3394.1 cm^{-1} due to the N--H bond stretching [21] was determined. This can be attributed to that these carboxyl groups have been coordinated into SBU structures to form the coordination polymer. The strong bands below 450 cm^{-1} in the MOF spectrum refer to the presence of $\text{Zn--O}/\text{Zn--N}$ coordination bonds [22]. The bands in the range of $1700\text{--}1400\text{ cm}^{-1}$ represent the stretching of $\text{C=O}/\text{C=N}/\text{C=C}$ bonds in both samples. Similarly, bands in the range of $1400\text{--}1200\text{ cm}^{-1}$ can be assigned to the stretching of $\text{C--O}/\text{C--N}/\text{C--C}$ bonds and the bending of --CH_2 and --CH_3 groups [21]. The two medium bands in the MOF spectrum at ~ 2360 and $\sim 2340\text{ cm}^{-1}$ refer to the asymmetric stretching of the adsorbed CO_2 (CO_2 double band) [23].

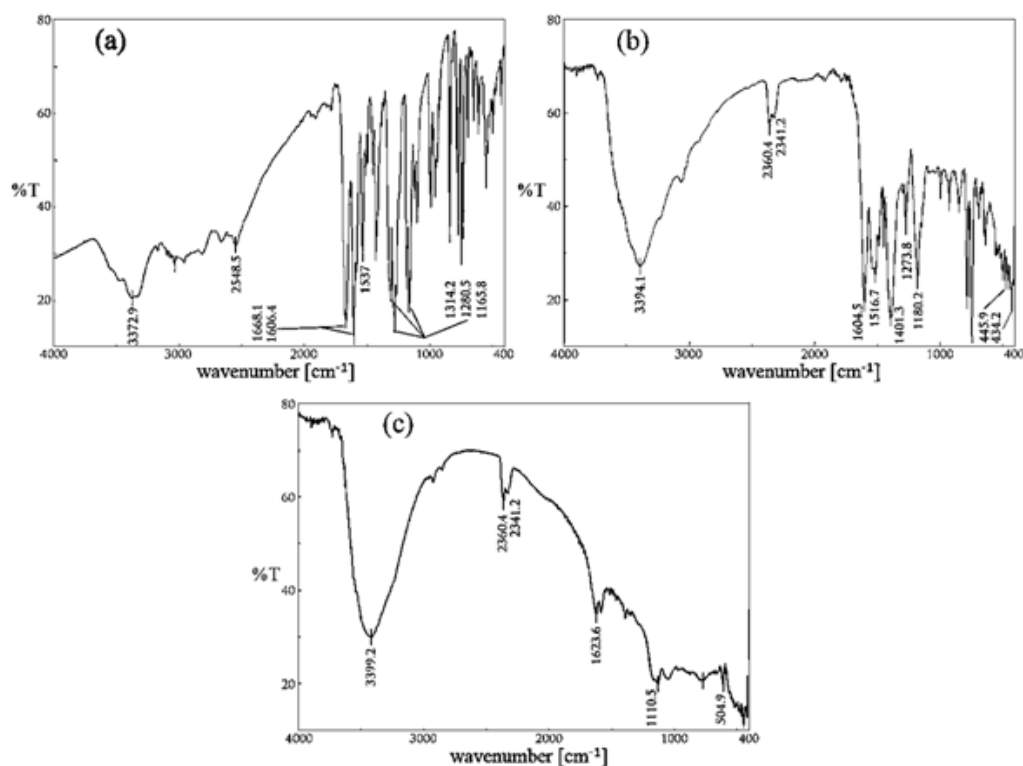


Fig. 2. FTIR spectra of (a) BMAB organic ligand, (b) the synthesized MOF and (c) the degradation product in alkaline solution

Diffuse reflection spectra in the UV range (UV-DRS) were observed using Shimadzu densitometer for samples of inactivated and activated MOF (Fig. 3-a) by spreading small amounts of the dry, ground materials on a glass plate and putting it into the instrument. These spectra along with the Kubelka-Munk function patterns (Fig. 3-b) were used as a complementary characterizing method and to confirm the success of desolvation process.

$$F(R) = \frac{K}{S} = \frac{(R-1)^2}{2R} \quad (1)$$

Equation 1 represents the Kubelka-Munk function, where K and S refer to the absorption coefficient [Cm^{-1}], and the scattering coefficient [Cm^{-1}]; respectively, and R is the detected diffuse reflectance [18]. According to this equation, an increase in the scattering coefficient corresponds to a decrease in F(R) value, and that is why the F(R) function decreased significantly for the activated MOF sample in comparison with the inactivated form, as the guest molecules removal during the activation process increased the surface area and pore volumes thus increasing the scattering coefficient. This effect of activation process on F(R) value was not observed at wave lengths below 250 nm. This could be due to the high absorptivity of the guest solvent (DMF) in this range [24], which caused significant decrease in K value upon activation. The DRS spectra were used successfully as a characterizing technique, as they showed high repeatability between batches for both activated and inactivated MOF samples.

Thermal characteristics were observed by differential scanning calorimetry (DSC) in the range 75–375°C with a heating rate of 10°C/min (Fig. 4). By comparing DSC patterns before and after activation, the success of activation process can be confirmed. An endothermic peak was determined for the inactivated MOF sample at 306.9°C. This peak represents the desolvation process as it was not observed for the activated sample. In addition, it is accompanied by a significant weight loss according to "Loss on Desolvation" measurements. The several random peaks after 306.9°C in the DSC pattern of inactivated material indicate framework collapse after guest solvent removal. These peaks were not observed in the activated MOF sample, which confirms the importance of using solvent-exchange protocol for the activation

process and suggesting better thermal stability for the activated MOF structure.

"Loss on desolvation" measurement was employed to determine the weight percentage (w%) of DMF in the synthesized MOF. Three 25 mg samples were put at 310°C under inert conditions for 1 hr., and then the residual weight of the samples was detected. The mean percentage of weight loss in the samples was 18.584%.

Zinc ions concentrations in samples from MOF material before and upon activation were determined using atomic absorption spectroscopy. Samples were digested in $\text{HNO}_3:\text{H}_2\text{O}_2$ (4:1, v/v) solution, and then diluted to the appropriate linear range. Average Zn% (g/100 g) values were 15.895% and 19.364% for the inactivated and activated MOF; respectively.

Both substituted benzotriazole and the carboxyl moiety in BMAB structure (Fig. 1) act as bis-monodentate ligand with Zn atoms. Therefore, the synthesized MOF has one of the chemical structures shown in Table 1. By comparing the detected Zn%-value using AAS and the calculated Zn%-value for each proposed structure in Table 1, the chemical composition of the synthesized MOF can be confirmed to be $[\text{Zn}(\text{BMAB})_2\text{DMF}]_n$.

Specific Surface Area (SSA) of the activated MOF was determined using Langmuir isotherm of the absorption of methylene blue (MB) [25]. The linear Langmuir equation type 1 (Eq.2), and SSA equation (Eq.3) were employed for this purpose.

$$\frac{C_{\text{eq}}}{q_{\text{eq}}} = \left(\frac{1}{q_m}\right) C_{\text{eq}} + \frac{1}{Kq_m} \quad (2)$$

$$\text{SSA} = \frac{q_m \times N \times A}{1000 \times M_w} \quad (3)$$

C_{eq} (mg/L) is the equilibrium concentration of MB, q_{eq} and q_m (mg/g) are the amount of MB adsorbed by 1g of the stationary phase at the equilibrium, and when a full monolayer of MB is formed; respectively, K is the equation constant, N is Avogadro's number ($6.019 \times 10^{23} \text{ mol}^{-1}$), A is the surface area occupied by one molecule of MB (197.2 \AA^2), and M_w (g/mol) is the molecular weight of MB.

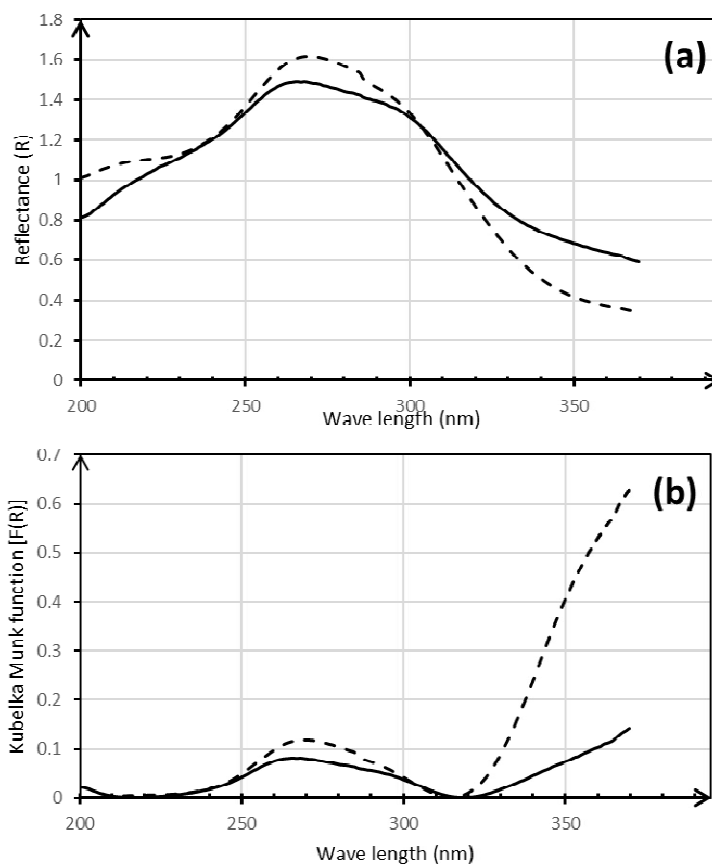


Fig. 3. (a) UV diffuse reflection spectra and (b) Kubelka-Munk function patterns of the synthesized MOF. [Dotted and solid lines are for inactivated and activated structures; respectively]

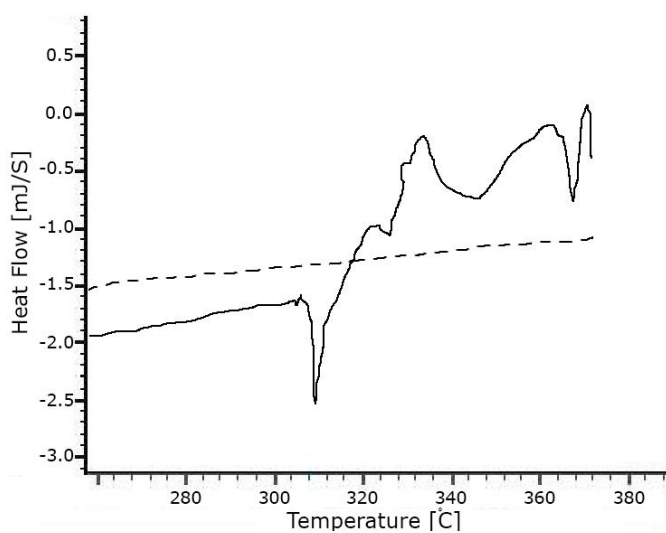


Fig. 4. DSC curve of inactivated (solid line), and activated (dotted line) MOF. The scale was minimized for clarity

Table 1. The potential structures of the synthesized MOF depending on the favorable linkage capacity of zinc and the organic linker

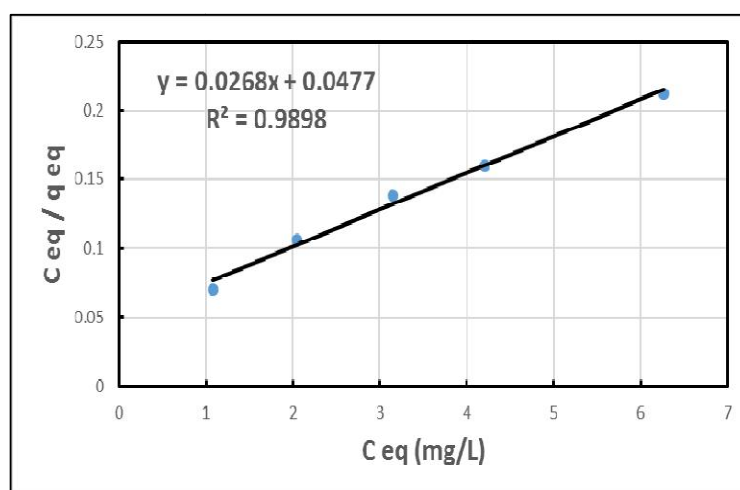
Possible structure [L=BMAB]	M _w of the activated structure	W% (g/100 g) of the activated structure	n	Calculated W% (g/100 g) of zinc in the inactivated structure
Zn ₄ O[L] ₃ .nDMF	1082.33	(100-18.584)	3.3801	19.672
Zn ₃ [OH][L] _{2.5} .nDMF	838.815	=81.416	2.6196	19.037
Zn ₅ [OH] ₂ [L] ₄ .nDMF	1433.98		4.4783	18.560
Zn ₆ [OH] ₄ [L] ₄ .nDMF	1533.36		4.7886	20.828
Zn[L].nDMF	333.65		1.0419	15.953

Several concentrations of methylene blue in distilled water were prepared in the range of 40–80 mg/L. 0.2% of PVP 30 was added as a suspending agent. 25 mg of the activated MOF was suspended in 10 mL of each of the previous solutions with frequent shaking for 6 hrs. to reach the equilibrium state. C_{eq} and q_{eq} values were spectrophotometrically determined at 665 n.m. for the centrifuged suspensions. The linear plot (Eq.2) was drawn according to the observed data (Fig. 5). q_m value was then determined as 37.31 mg/g, and applied to the SSA equation (Eq.3). By comparing the physical characteristics of the methylene blue powder used in this work with the different types of methylene blue hydrate determined by Rager et al. [26], our methylene blue is the Type-B hydrate with a mean molecular weight of ~360.35 g/mol. The calculated specific surface area of the activated MOF is 122.90 m²/g. The other three types of Langmuir equation were also used and showed quite similar results as SSA values were in the range of 110.16–122.90 m²/g.

3.2 Chromatographic Evaluation of [Zn(BMAB)]_n

The properties of the activated MOF as a TLC stationary phase was studied. UV-DRS spectra were recorded for the prepared plates, which were identical to the previously observed spectrum of the MOF upon activation, confirming that the preparation process of TLC plates does not affect the activated structure.

The prepared mixture of benzidine and o-tolidine was successfully separated on [Zn(BMAB)]_n-coated TLC plates using the abovementioned mobile phase, as two separated blue spots were produced after incubation in the iodine chamber (Fig. 6-b). The retardation factors (R_f) were densitometrically determined (Fig. 6-a) before iodine visualization at a wave length of 310 nm to be 0.45 and 0.63 for o-tolidine and benzidine; respectively. The calculated separation factor, and resolution were α=2.08, and R_S=1.61.

**Fig. 5. Linear plot of Langmuir equation type-1 of the absorption of methylene blue on the activated MOF**

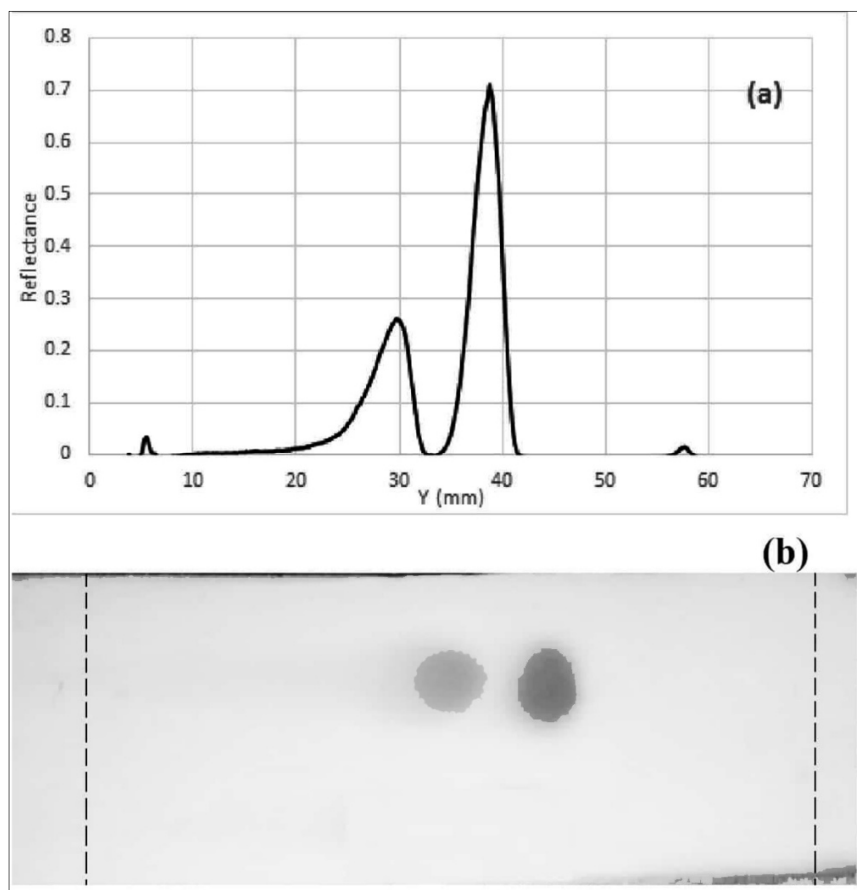


Fig. 6. (a) densitogram, and (b) iodine visualization of the separated mixture of benzidine, o-tolidine on $[Zn(BMAB)]_n$ -coated TLC plate using n-propanol:chloroform:acetonitrile (50:30:20, v/v/v) as mobile phase system

Both benzidine and o-tolidine consist of hydrophobic biphenyl structure (Fig. 7), but with primary amine groups which can play as π acceptors. These two reasons could explain why both structures have a moderate retention on the hydrophobic $[Zn(BMAB)]_n$ stationary phase.

However, o-tolidine is substituted with two methyl groups making it less polar, and then may experience slightly stronger retention on the stationary phase and less elution by the polar mobile phase, which illustrates the ability of this chromatographic system to separate the mixture.

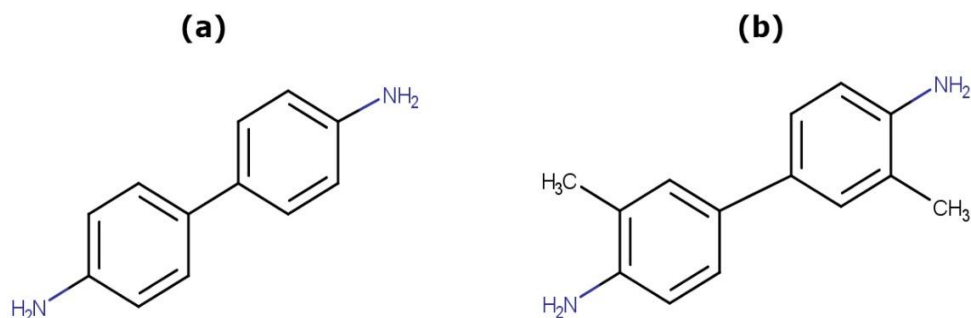


Fig. 7. The chemical structure of (a) Benzidine, and (b) o-Tolidine

4. CONCLUSION

A new Zn-based MOF structure consists of a bidentate organic linker with chemically distinct binding groups was synthesized and characterized in this study. The chromatographic evaluation of the synthesized $[Zn(BMAB)]_n$ was conducted using TLC, as it is considered a simple, easy-to-prepare technique. This evaluation confirmed the ability of this stationary phase to separate a model mixture of aromatic amines. However, the high surface area and permanent porosity in up to 375°C of the activated form of this MOF material make it a potential stationary phase for Gas Chromatography. Besides, the exceptional hydrophobic characteristic of $[Zn(BMAB)]_n$ make it possible for this material to be used in the cartridges of Reversed-Phase Solid Phase Extraction (RP-SPE). More studies are needed to explore the beneficial characteristics of these materials in Analytical Chemistry applications.

DISCLAIMER

The products used for this research are commonly and predominantly use products in our area of research and country. There is absolutely no conflict of interest between the authors and producers of the products because we do not intend to use these products as an avenue for any litigation but for the advancement of knowledge. Also, the research was not funded by the producing company rather it was funded by personal efforts of the authors.

ACKNOWLEDGEMENTS

The authors thank Dr. Wassim Abdelwahed, Dr. Lama Alchab, and Dr. Firas Nahas for helpful discussions.

COMPETING INTERESTS

Authors have declared that no competing interests exist.

REFERENCES

- Jork H, Funk W, Fischer W, Wimmer H. Thin-layer chromatography reagents and detection methods. (Translated version by: Hampson, F., Hampson, J.A.). VCH Verlagsgesellschaft rabH, Weinheim, Germany. 1990;1a.
- Vanhaelen M, Vanhaelen-Fastré R. Thin-layer chromatography-densitometry as a powerful method for the standardization of medicinal plant extracts. In: Dallas FAA, Read H, Ruane RJ, Wilson ID, editors. Recent Advances in Thin-Layer Chromatography. Boston MA: Springer; 1988
Available: https://doi.org/10.1007/978-1-4899-2221-2_20
- Zhang J, Chen Z. Metal-organic frameworks as stationary phase for application in chromatographic separation, J Chromatogr A. 2017;1530:1–18.
Available: <https://doi.org/10.1016/j.chroma.2017.10.065>
- Yaghi OM, Kalmutzki MJ, Diercks CS. Introduction to reticular chemistry: Metal-organic frameworks and covalent organic frameworks. 1st ed. Weinheim: Wiley-VCH; 2019.
Available: <https://doi.org/10.1002/9783527821099>
- Kitagawa S, Kitaura R, Noro S. Functional porous coordination polymers. Angew Chem Int Ed. 2004;43(18):2334–2375.
Available: <https://doi.org/10.1002/anie.200300610>
- Tranchemontagne DJ, Park KS, Furukawa H, Eckert J, Knobler CB, Yaghi OM. Hydrogen storage in new metal-organic frameworks. J Phys Chem C. 2012; 116(24):13143–13151.
Available: <https://doi.org/10.1021/jp302356q>
- Tu B, Pang Q, Ning E, Yan W, Qi Y, Wu D, Li Q. Heterogeneity within a mesoporous metal-organic framework with three distinct metal-containing building units. J Am Chem Soc. 2015;137(42):13456–13459.
Available: <https://doi.org/10.1021/jacs.5b07687>
- Pacheco-Fernández I, González-Hernández P, Pasán J, Ayala JH, Pino V. The rise of metal-organic frameworks in analytical chemistry. In: de la Guardia M, Esteve-Turrillas FA, editors. Handbook of Smart Materials in Analytical Chemistry, 1st ed. Hoboken: John Wiley & Sons Ltd; 2019.
Available: <https://doi.org/10.1002/9781119422587.ch15>
- Yang CX, Zheng YZ, Yan XP. γ -Cyclodextrin metal-organic framework for efficient separation of chiral aromatic alcohols. RSC Adv. 2017;7(58):36297–36301.

- Available:<https://doi.org/10.1039/C7RA06558B>
10. Qu Q, Xuan K, Zhang K, Chen X, Ding Y, Feng S, Xu Q. Core-shell silica particles with dendritic pore channels impregnated with zeolite imidazolate framework-8 for high performance liquid chromatography separation. *J Chromatogr A*. 2017;1505:63–68.
Available:<https://doi.org/10.1016/j.chroma.2017.05.031>
 11. Ehrling S, Kutzscher C, Freund P, Müller P, Senkovska I, Kaskel S. MOF@SiO₂ core-shell composites as stationary phase in high performance liquid chromatography. *Micropor Mesopor Mat*. 2018;263:268–274.
Available:<https://doi.org/10.1016/j.micromeso.2018.01.003>
 12. Tanaka K, Kawakita T, Morawiak M, Urbanczyk-Lipkowska Z. A novel homochiral metal–organic framework with expanded open cage based on (R)-3,3'-bis(6-carboxy-2-naphthyl)-2,2'-dihydroxy-1,1'-binaphthyl: Synthesis, X-ray structure and efficient HPLC enantiomer separation. *CrystEngComm*. 2019;21:487–493.
Available:<https://doi.org/10.1039/c8ce01791c>
 13. Xie SM, Zhang XH, Wang BJ, Zhang M, Zhang JH, Yuan LM. 3D chiral nanoporous metal–organic framework for chromatographic separation in GC. *Chromatographia*. 2014;77:1359–1365.
Available:<https://doi.org/10.1007/s10337-014-2719-4>
 14. Wu YY, Yang CX, Yan XP. An in situ growth approach to the fabrication of zeolite imidazolate framework-90 bonded capillary column for gas chromatography separation. *Analyst*. 2015;140:3107–3112.
Available:<https://doi.org/10.1039/C5AN00077G>
 15. Xue XD, Zhang M, Xie SM, Yuan LM. Homochiral metal-organic framework [Zn₂(D-cam)₂(4,4'-bpy)]_n for high-resolution gas chromatographic separations. *Acta Chromatogr*. 2015;27:15–26.
Available:<https://doi.org/10.1556/AChrom.27.2015.1.2>
 16. Yang X, Li C, Qi M, Qu L. Graphene-ZIF8 composite material as stationary phase for high-resolution gas chromatographic separations of aliphatic and aromatic isomers, *J Chromatogr A*. 2016;1460:173–180.
Available:<https://doi.org/10.1016/j.chroma.2016.07.029>
 17. Schenk C, Kutzscher C, Drache F, Helten S, Senkovska I, Kaskel S. Metal–Organic Frameworks for Thin-Layer Chromatographic Applications. *ACS Appl Mater Interfaces*. 2017;9(3):2006–2009.
Available:<https://doi.org/10.1021/acsami.6b13092>
 18. Melero JA, Iglesias J, Sáinz-Pardo J, Arsuaga JM. Synthesis of titanium containing periodic *Mesoporous organosilica*. *Stud Surf Sci Catal*. 2007;170:450–455.
Available:[https://doi.org/10.1016/S0167-2991\(07\)80875-5](https://doi.org/10.1016/S0167-2991(07)80875-5)
 19. AlShaghel A. Benzotriazole condensation reactions with some primary aromatic amines derivatives in the presence of formaldehyde under the influence of ultrasound [in Arabic], *Research Journal of Aleppo University - Basic Science Series*. 2018;124:1–14.
 20. Howarth AJ, Peters AW, Vermeulen NA, Wang TC, Hupp JT, Farha OK. Best Practices for the Synthesis, Activation, and Characterization of Metal–Organic Frameworks. *Chem. Mater*. 2016;29(1):26–39.
Available:<https://doi.org/10.1021/acs.chemmater.6b02626>
 21. Coates J. Interpretation of Infrared Spectra: A Practical Approach. In: Meyers RA, editor. *Encyclopedia of Analytical Chemistry*. New York: John Wiley & Sons Ltd; 2006.
Available:<https://doi.org/10.1002/9780470027318.a5606>
 22. Uysal I, Severcan F, Evis Z. Characterization by Fourier transform infrared spectroscopy of hydroxyapatite co-doped with zinc and fluoride. *Ceram Int*. 2013;39(7):7727–7733.
Available:<https://doi.org/10.1016/j.ceramint.2013.03.029>
 23. Stevens RW, Siriwardane RV, Logan J. *In situ* fourier transform infrared (ftir) investigation of CO₂ adsorption onto zeolite materials. *Energy Fuels*. 2008;22(5):3070–3079.
Available:<https://doi.org/10.1021/ef800209a>
 24. Talrose V, Stern EB, Goncharova AA, Messineva NA, Trusova NV, Efimkina MV. UV/Visible spectra. In: Linstrom PJ, Mallard WG, editors. *NIST Chemistry WebBook, Standard Reference Database*

- Number 69. Gaithersburg MD: National Institute of Standards and Technology. 20899; 2018.
(Retrieved April 5, 2020)
Available:<https://doi.org/10.18434/T4D303>
25. Itodo AU, Itodo HU, Gafar MK. Estimation of Specific Surface Area using Langmuir Isotherm Method. J Appl Sci Environ Manage. 2010;14(4):141–145.
Available:<https://doi.org/10.4314/jasem.v14i4.63287>
26. Rager T, Geoffroy A, Hilfiker R, Storey JMD. The crystalline state of methylene blue: A zoo of hydrates. Phys Chem Chem Phys. 2012;14(22):8074–8082.
Available:<https://doi.org/10.1039/C2CP40128B>

© 2020 Rasheed et al.; This is an Open Access article distributed under the terms of the Creative Commons Attribution License (<http://creativecommons.org/licenses/by/4.0>), which permits unrestricted use, distribution, and reproduction in any medium, provided the original work is properly cited.

Peer-review history:
The peer review history for this paper can be accessed here:
<http://www.sdiarticle4.com/review-history/58911>